2010 Thermal & Fluids Analysis Workshop

Methodology for the Assessment of 3D Conduction Effects In an Aerothermal Wind Tunnel Test

August 17, 2010

A. Brandon Oliver
brandon.oliver-1@nasa.gov

EG3: Applied Aeroscience and CFD Branch
National Aeronautics & Space Administration
Lyndon B. Johnson Space Center
Houston, TX 77058

Outline

- Problem
- Solution
- Results

Protuberance Heating Test (2007-Present)

Test objectives:

- Duplicate and extend 60's era test which is used for ET protuberance environments
- Obtain heating data useful for CFD model validation

Models:

- 11 different models of two-sided protuberances on a flat plate
- Protuberances mounted on a turn-table to permit varying cross-flow angle
- Instrumented with thin-film gages and pressure taps (4 models)

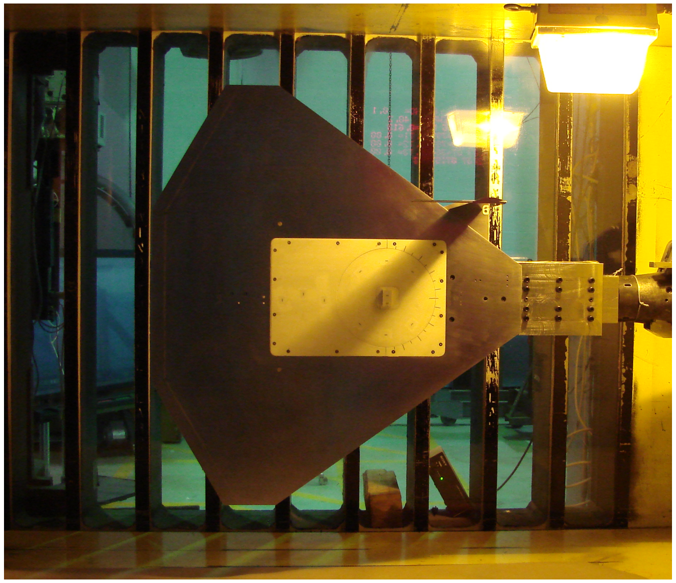

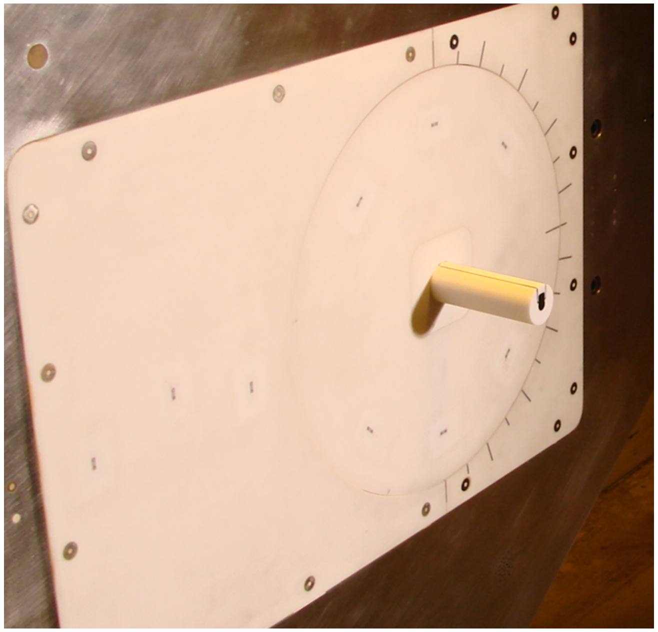

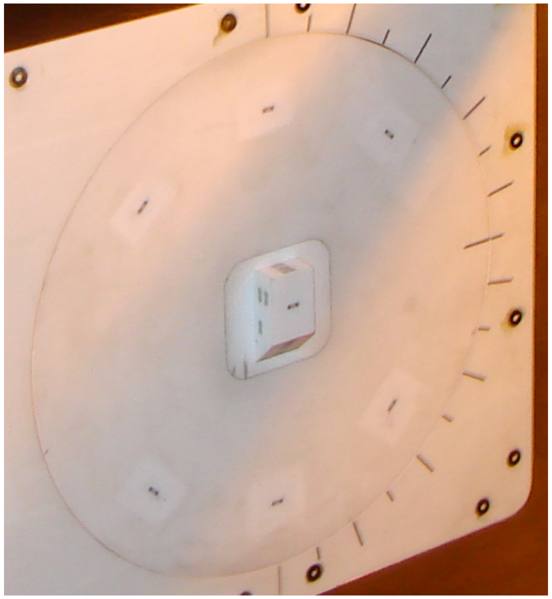

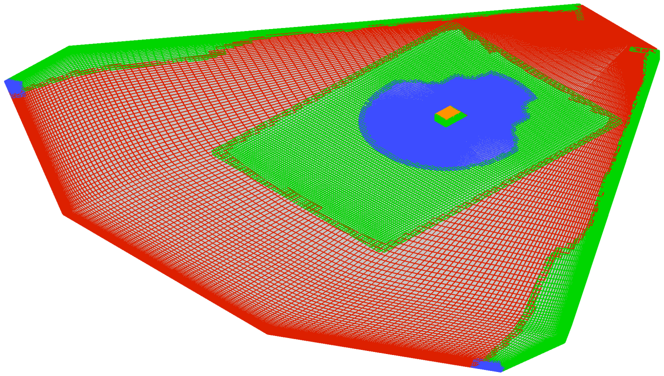

Possibly relevant test background

- **Run method:**
  - Model run in tunnel until temperatures come to a steady state (near adiabatic conditions)
  - Data acquisition begins
  - Heat pulse generated by bypassing a cooling unit in the tunnel circuit
  - Heat pulse drives heating which is measured by thin film gages
  - Heat pulse character a function of Mach number…development time varies from 5-12 seconds…run times vary from 20-35 seconds
  - Low thermal driving potential makes knowing the recovery factor important

1D vs. 3D Conduction Data Reduction Error

- **Extended run times of LaRC UPWT test method, along with small model size, permits heat to conduct farther and deeper into the model than in traditional aerothermal test facilities**
  - Thin-film reduction method assumes 1D conduction into semi-infinite slab
  - Actual test article has 3D geometric features and strong heating gradients

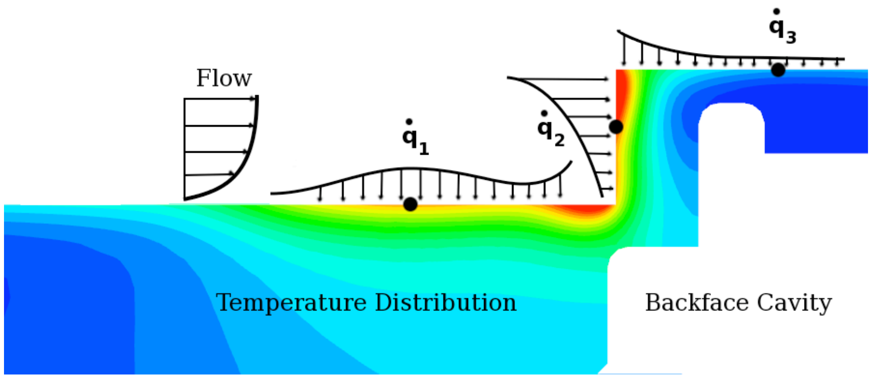

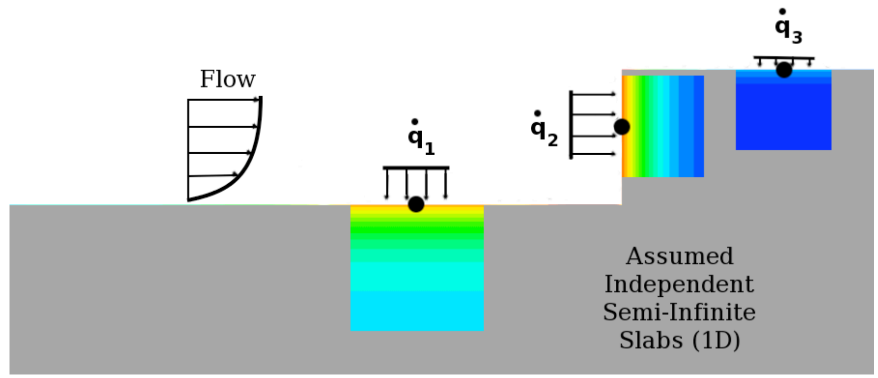

- **Goal of present effort:**
  - Identify protuberances and gages susceptible to this reduction error
  - Develop a process to quantify this error so that corrections may be applied

Analysis Process

Generic Testing and Reduction Process

With Specific Application to Thin-Film Measurement Technique

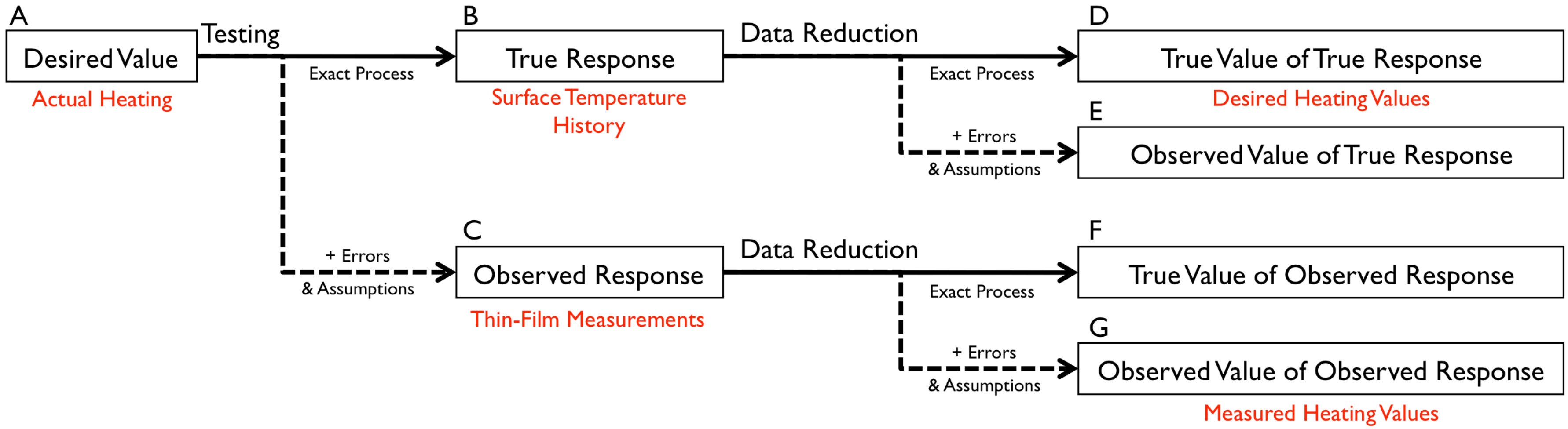

Testing Errors & Assumptions:
- Data Acquisition Errors
- Gage Interference

Reduction Errors & Assumptions:
- Cook-Felderman Assumptions:
  - 1D semi-infinite solid
  - Constant material properties
  - Constant heat transfer coefficient
- Data Filtering
- Measurement Errors in Freestream Conditions Used In Reduction

- **"3D conduction errors" are a data reduction error**
- **Have assessed conduction error using two different methods for defining the analytical 'actual' heating**
  - CFD – Brandon Oliver, JSC
  - Wind tunnel data correlations – Dr. Keith Woodbury, University of Alabama

CFD-Based Analysis Overview

Compressible Navier-Stokes CFD (OVERFLOW)

- Build grid
- Run solution at nominal pre-heat pulse freestream with adiabatic wall BCs to obtain recovery factor
- Re-converge solution with specified wall temperature BCs to obtain heat flux
- Combine results to obtain heat transfer coefficient distribution

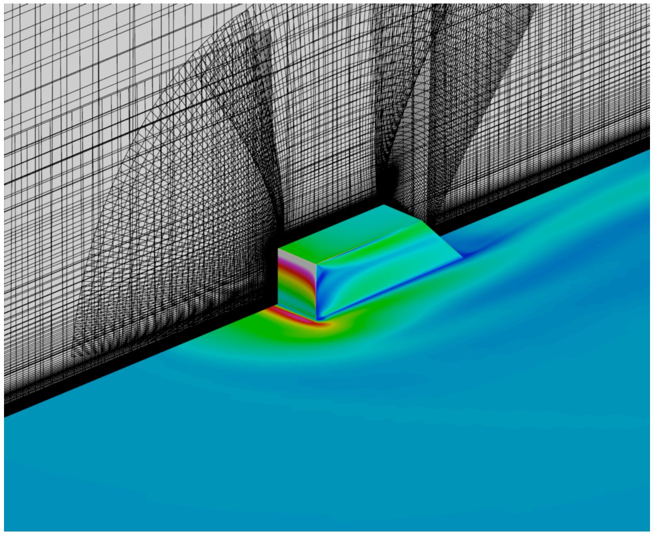

Finite-Element Thermal Model (FIN-S)

- Build grid
- Interpolate CFD recovery factor and heat transfer coefficient to thermal grid
- Run thermal model to steady state with pre-heat pulse total temperature to obtain initial thermal state
- Run heat pulse profile (taken from wind tunnel run data) to obtain surface temperature vs. time
- Process simulated surface temperature trace using Cook-Felderman
- Compare Cook-Felderman heating value (1D) with known, applied heating value (3D)

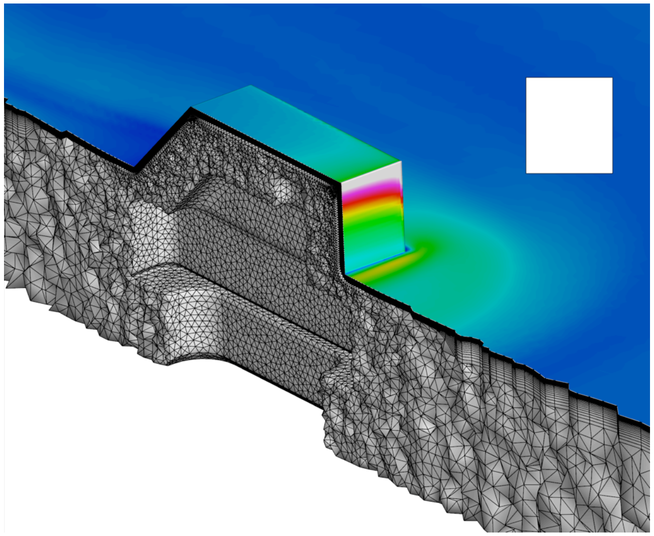

Code and Data Loose Coupling Method To Simulate a Wind Tunnel Run

CFD Solution for $StRe^{0.2}$

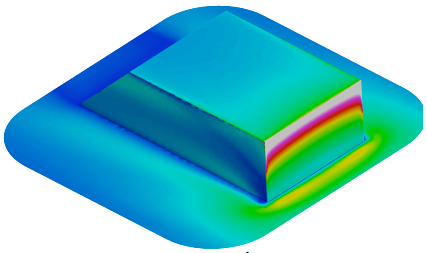

Tunnel measured flow conditions

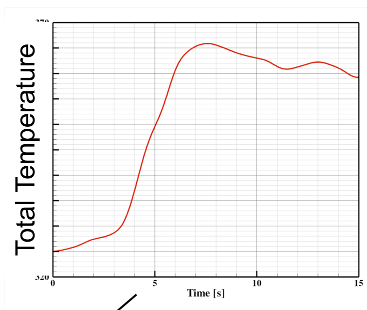

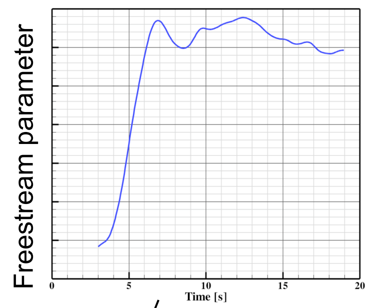

$$StRe^{0.2}\left(RT_o\left(t\right)-T_w\left(t\right)\right)\left(\frac{\rho_\infty U_\infty C_p}{Re^{0.2}}\right)=q''_w\left(t\right)$$

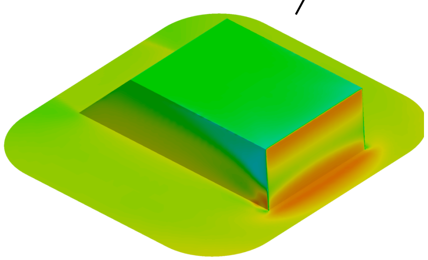

CFD Solution for recovery factor

Finite-Element Thermal Model

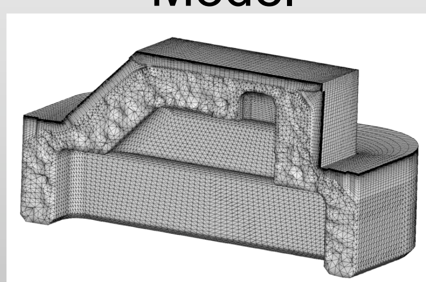

Simulated surface temperature history

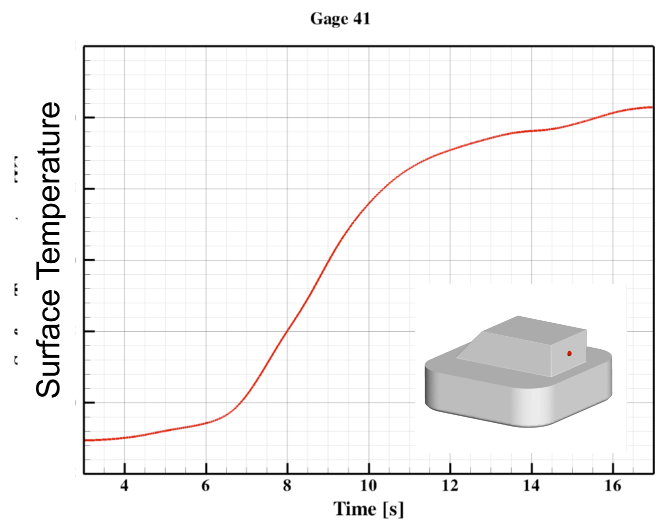

- **Thermal model yields surface temperature vs. time**
  - **Treat as 'simulated data'**

Compute “Adiabatic” Solution

- **Thermal solver is run to steady-state with the pre-heat pulse total temperature**

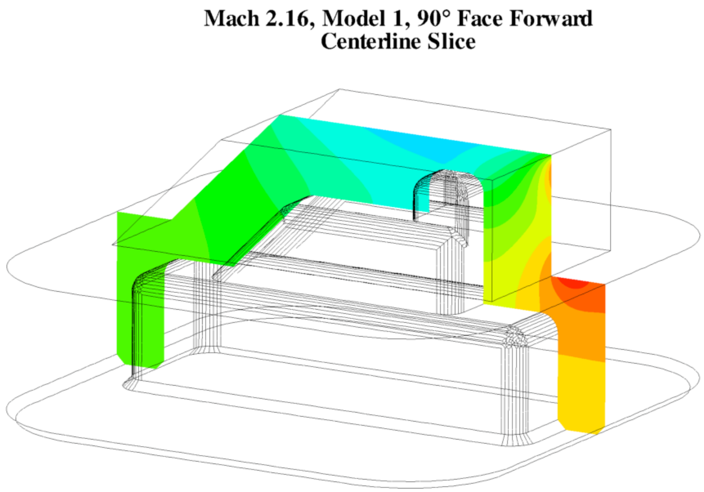

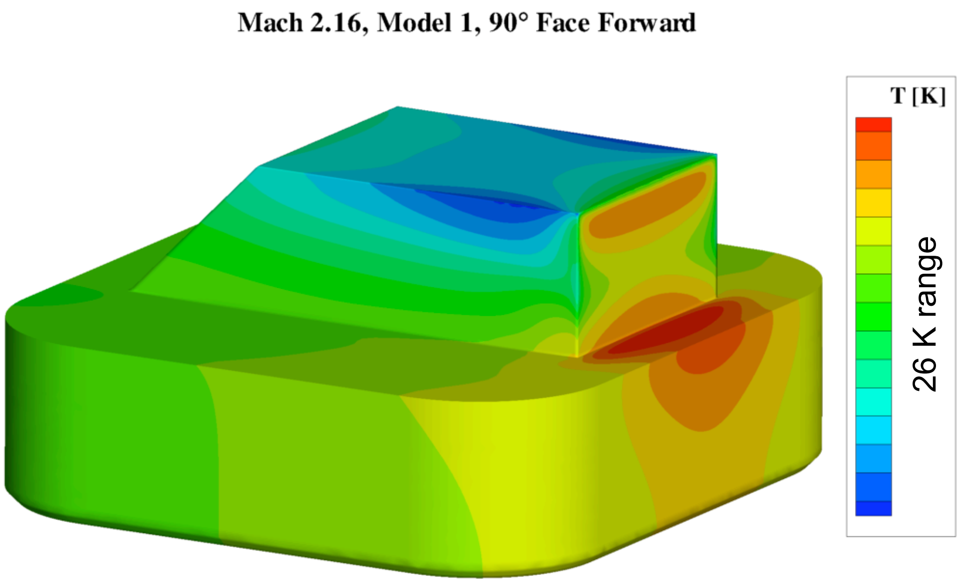

- **Yields the temperature distribution during the ‘adiabatic’ portion of the run**

Apply 1-D Reduction to Simulated Data

- **Apply the Cook-Felderman reduction to the simulated temperature trace provided by thermal model**

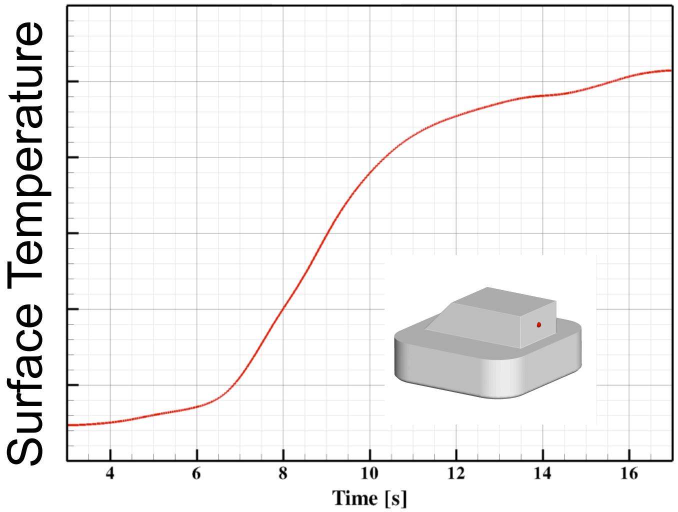

Cook-
Felderman
→

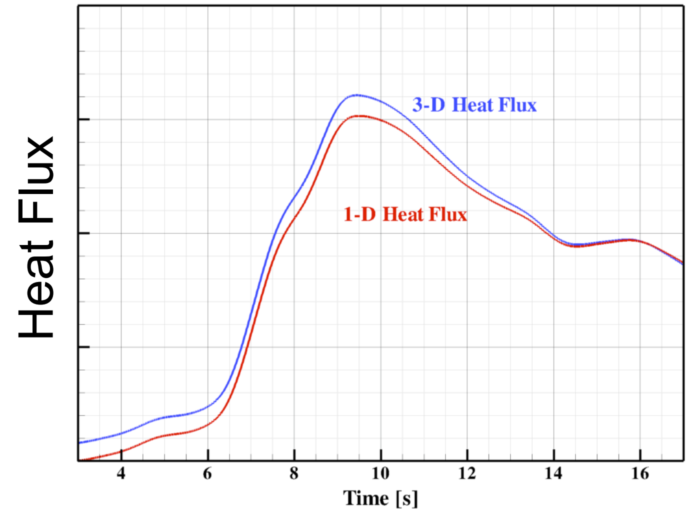

- **This “1-D conduction” result is equivalent to the measured thin-film results**
- **Compute error using heat transfer coefficient instead of heat flux**
  - Adiabatic wall temperature error scales out a good portion of the heat flux error

$$\text{1D Reduction Error } [\%] = 100 \cdot \frac{H_{Cook-Felderman} - H_{3D}}{H_{3D}}$$

  - Positive error: Test over-predicts actual heating

Model 1, CFANGLE 180, Mach 1.50, No Turntable

- **3D conduction effects:**
  - Higher ‘observed’ heating near corners
  - Washes out localized flow patterns
    - Cool streak on side of protuberance
    - Peak heating ahead of protuberance
  - Lower ‘observed’ heating near the base of the protuberance

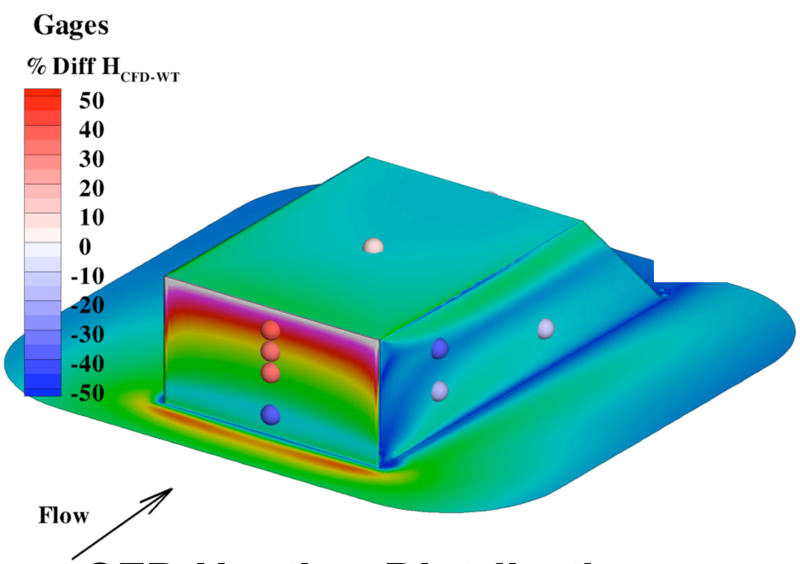

CFD Heating Distribution

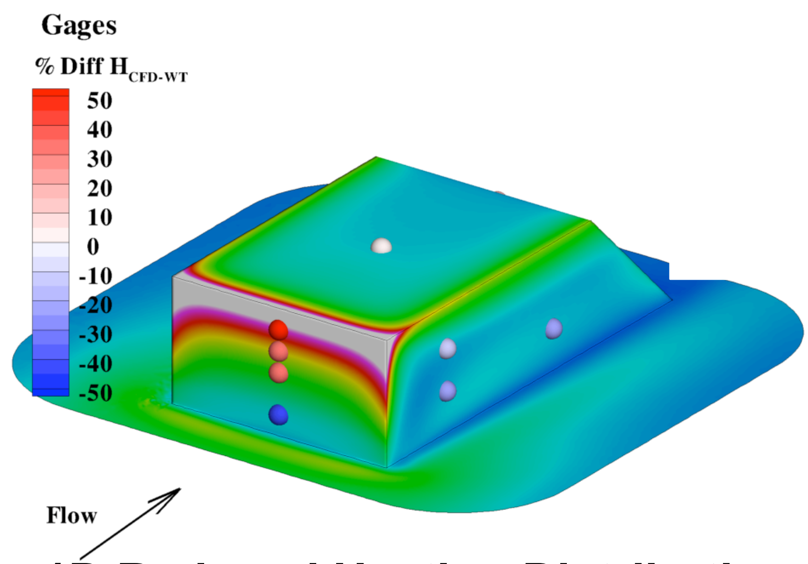

1D Reduced Heating Distribution

Model 1, CFANGLE 180, Mach 1.50, No Turntable

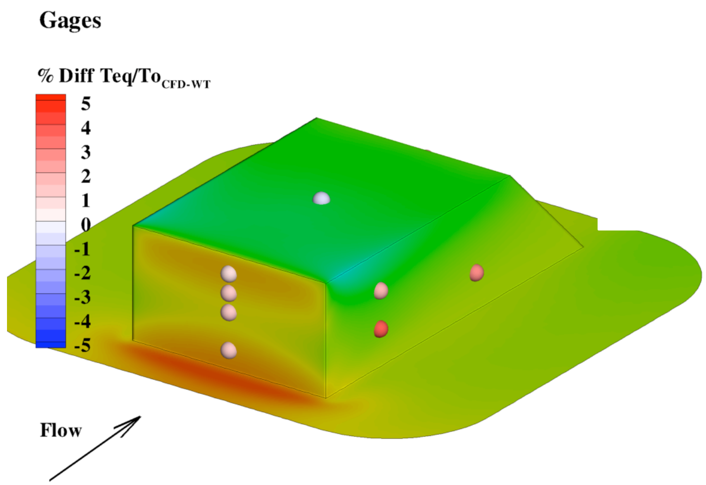

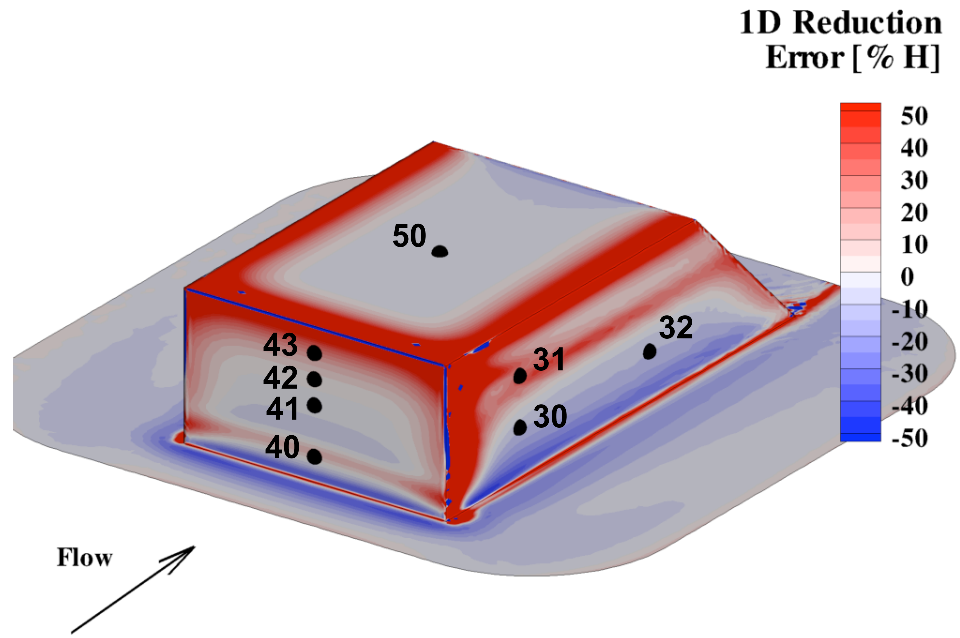

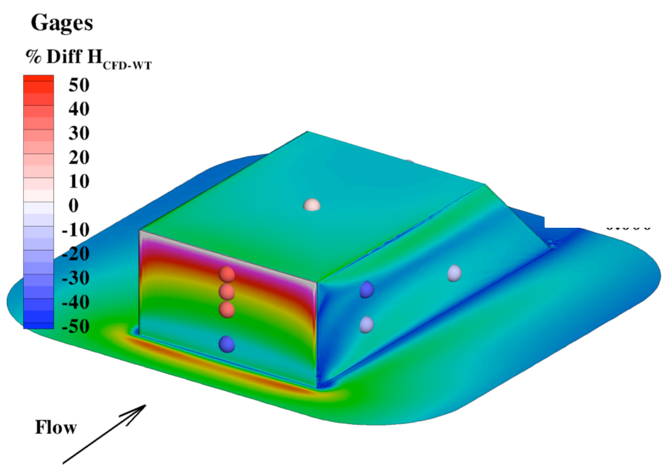

Solution Verification

- **Thermal model timestep convergence verified adequate ($\Delta t=0.05s$)**
- **Thermal model grid convergence**
  - Wall spacing and wall stretching ratio studied using flat plate with a peak heating heat transfer coefficient applied
  - Models 10 & 11, Mach 1.50 runs with doubled grid resolution in all directions in the near-wall structured zones
  - Model 9 & 10, Mach 2.16 compare qualitatively well with previous (much finer) grids
  - Model 1 without turntable grid independence established for several surface and in-depth grid distributions
- **CFD grid convergence**
  - Models 1 and 9, Mach 1.5 run with refined grids
    - Small differences were observed
    - Details in documentation
- **New CFD solutions generated with better wall spacing, but could still use work**
  - Several previous protuberance solutions did not meet best practices standards for wall spacing
  - Fine-spacing has introduced some noise into solutions

Grid Convergence

- **Verified wall spacing with semi-infinite slab model**
  - Applied peak protuberance heating uniformly to flat plate
  - Ran through a Mach 1.5 heat pulse
  - Identified that wall spacing of 0.001” provided grid independent 1D reduction error level
- **Flat plate solutions indicated -5% error due to constant material property assumption**
  - Verified with variable material property reduction using Chaleur & modified C-F to use temperature-dependent material properties

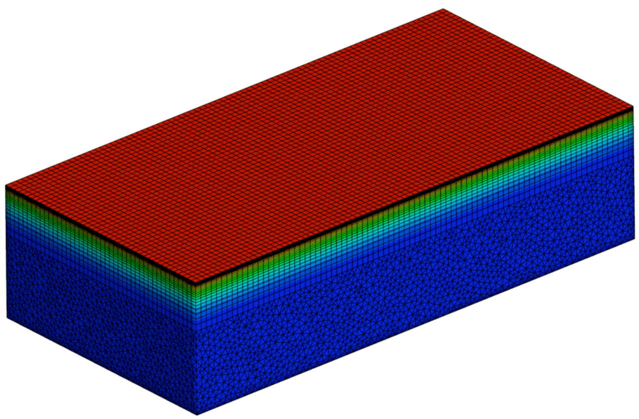

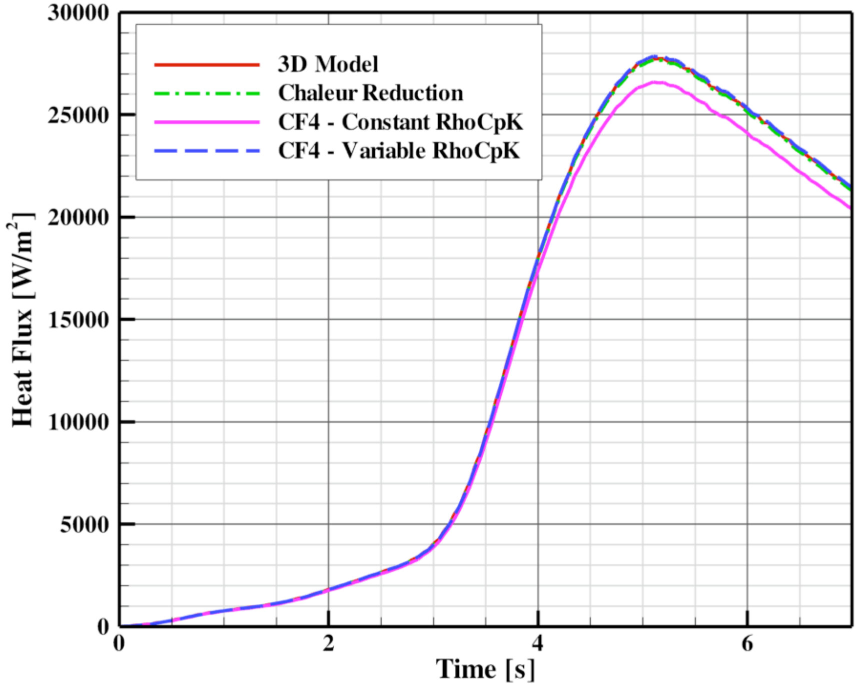

- Model 10, Mach 1.50
- Grid resolution refined in all directions in the near-wall structured zones

Baseline

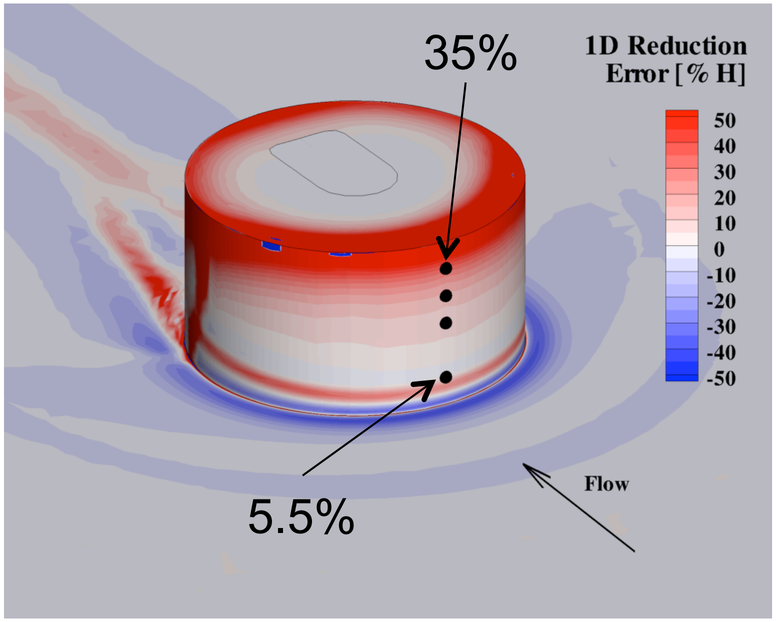

Refined

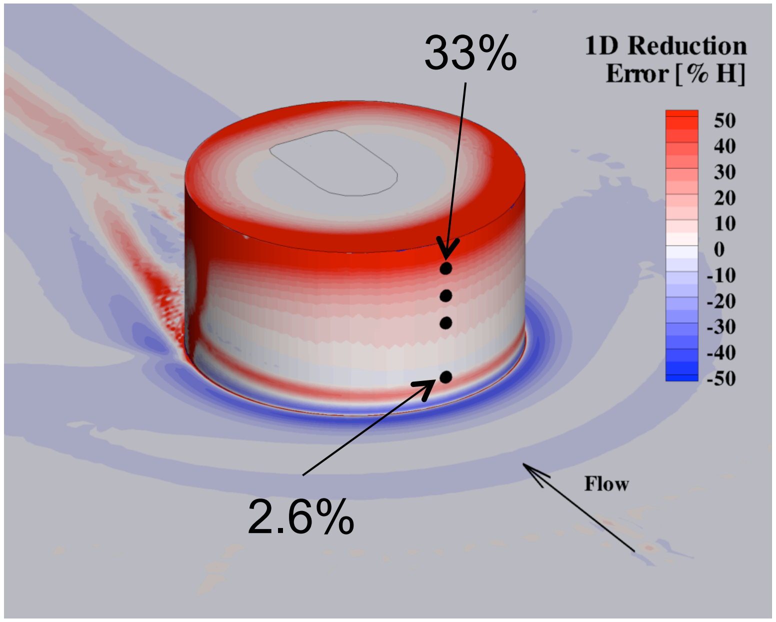

Grid Convergence

- **Model 11, Mach 1.50**
- **Grid resolution refined in all directions in the near-wall structured zones**

Baseline

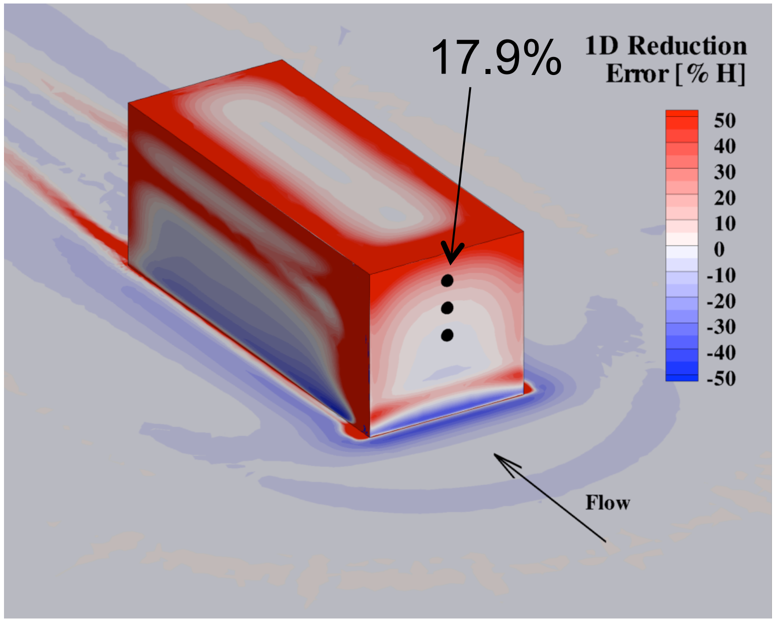

Refined

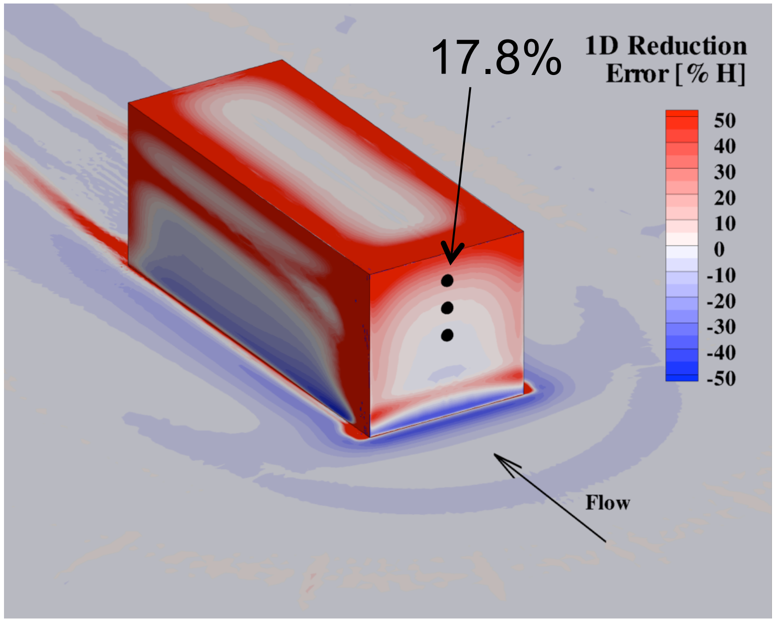

Mach Number Trend

- **Flow conditions favor higher dimensional heat flux for lower Mach numbers, leading to trend of decreasing error with Mach**
- **Extended time of test section 2 heat pulse causes increase in errors for Mach 3.51 runs (20 sec vs 10 sec)**

Mach 1.50

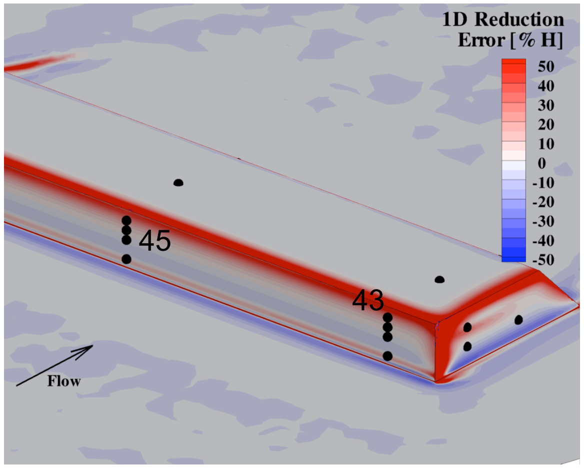

Gage 43: 27%
Gage 45: -2.3%

Mach 2.16

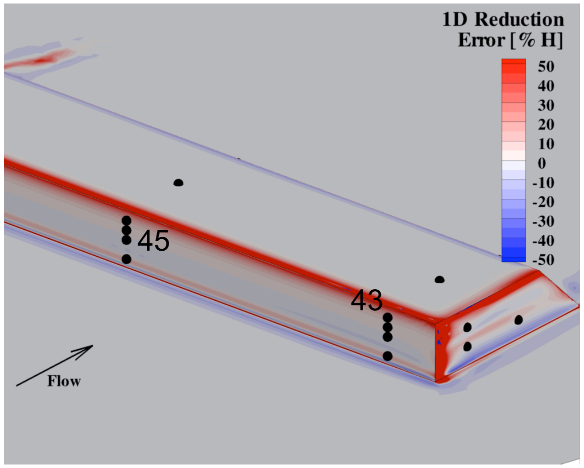

Gage 43: 12%
Gage 45: -1.3%

Mach 3.51

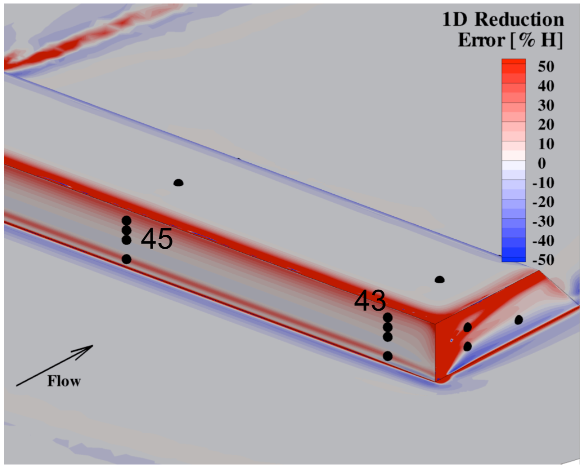

Gage 43: 20%
Gage 45: 1.1%

- **Trend consistent on Models 9 & 10**

Size Trends

- **Errors remain concentrated at corners**
- **Lower heating on shorter protuberance does not reduce percent error**

Model 4	**Model 1**	**Model 11**
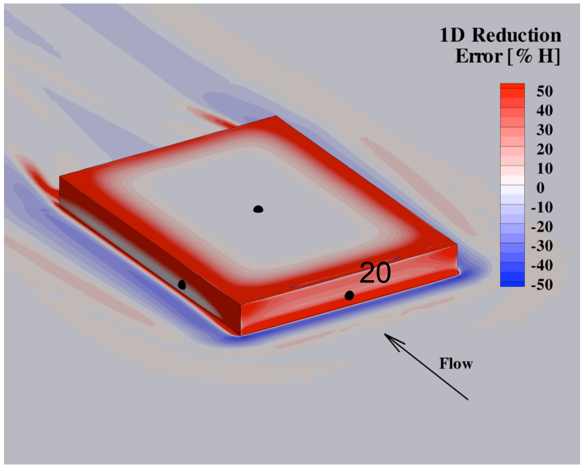	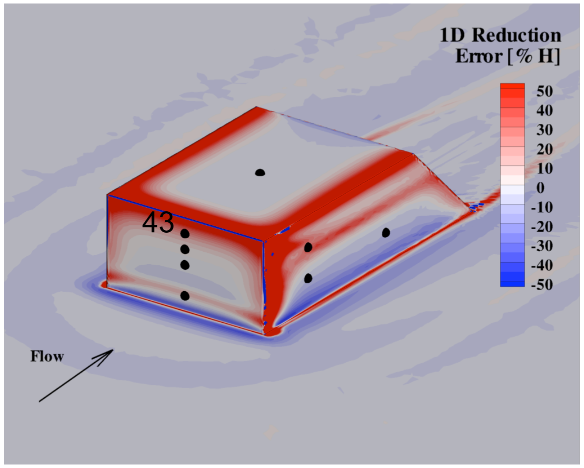	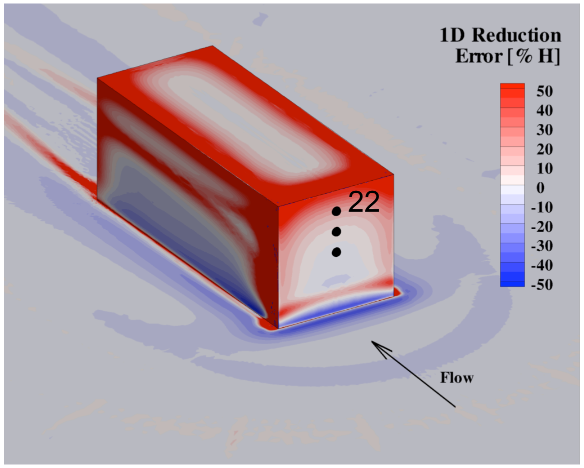
Highest Face Gage H ~ 23% Model 1 Error: 39%	Highest Face Gage H = Model 1 Error: 22%	Highest Face Gage H ~ 102% Model 1 Error: 18%

Model 1 Cross Flow

- **Cross flow does not significantly alter extent of errors from corners**
- **May not have to analyze all runs to determine correction factors**

CFANGLE 180

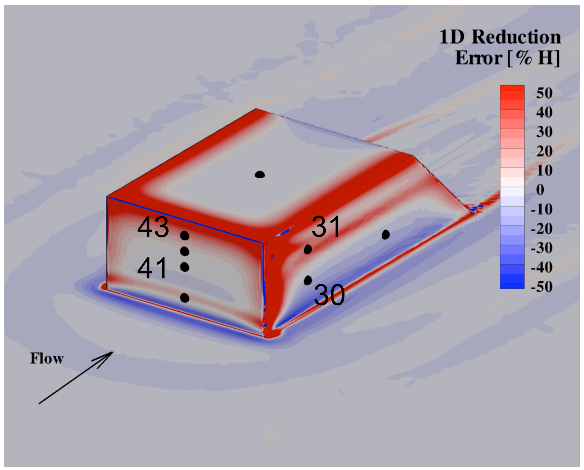

Gage 30: -7.6%
Gage 31: 26%
Gage 41: -2.6%
Gage 43: 22%

CFANGLE 120

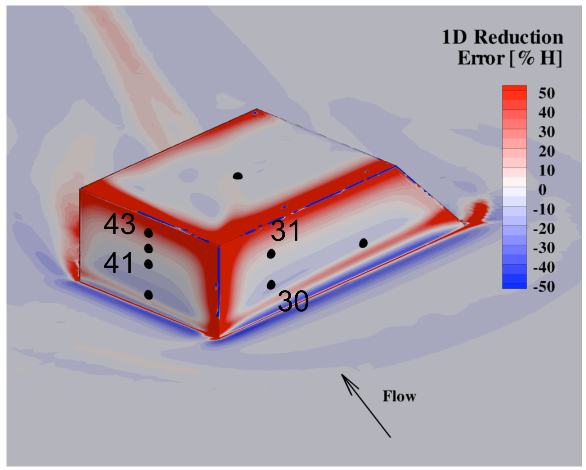

Gage 30: -8.6%
Gage 31: 3.2%
Gage 41: -3.2%
Gage 43: 32%

CFANGLE 90

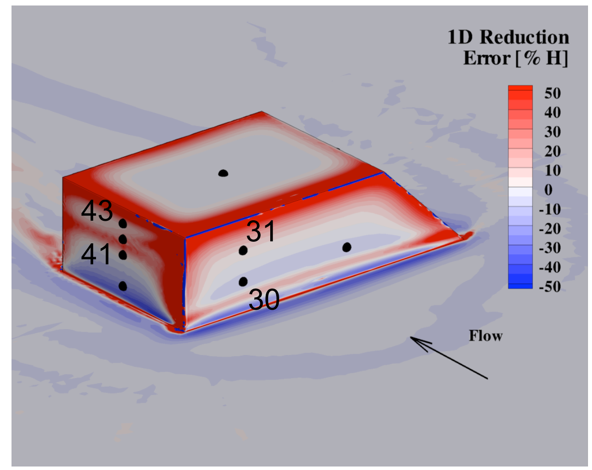

Gage 30: -8.5%
Gage 31: 5.1%
Gage 41: 9.0%
Gage 43: 14%

Model 6 Corner Gages

- **Corner gages strongly affected by 3D effects**
- **Currently working to assess if improved heat flux numbers can be obtained by using cylindrical coordinates in corner thin-film reduction**

CFANGLE 180

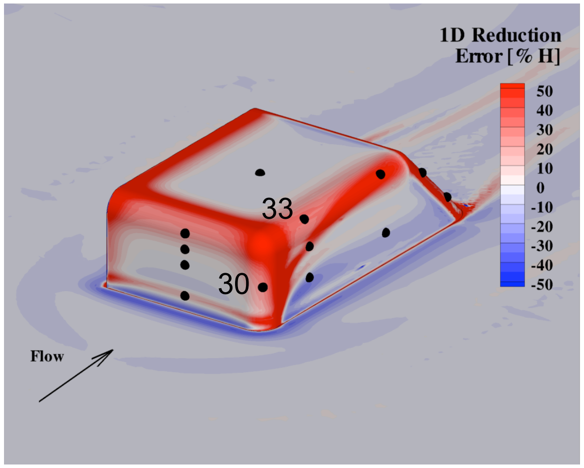

CFANGLE 120

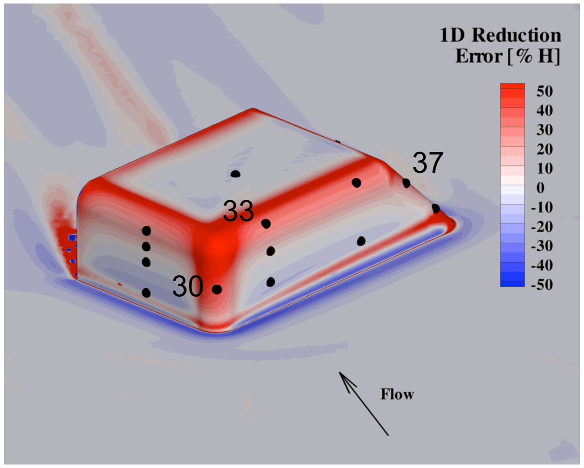

CFANGLE 30

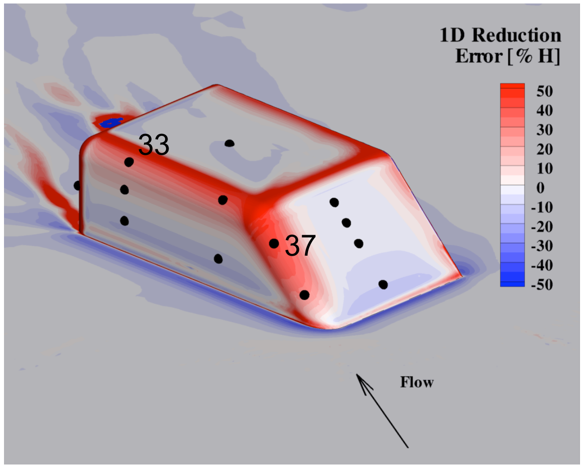

Gage 30: 25%
Gage 33: 30%

Gage 30: 40%
Gage 33: 31%
Gage 37: 25%

Gage 33: 32%
Gage 37: 41%

Don't forget: Red contours indicate tunnel data is over-conservative

Model 1 Peer Review Requests

- Turntable has negligible effect on model error
- 45 degree sloped face shows less error than 90 degree face

With Turntable

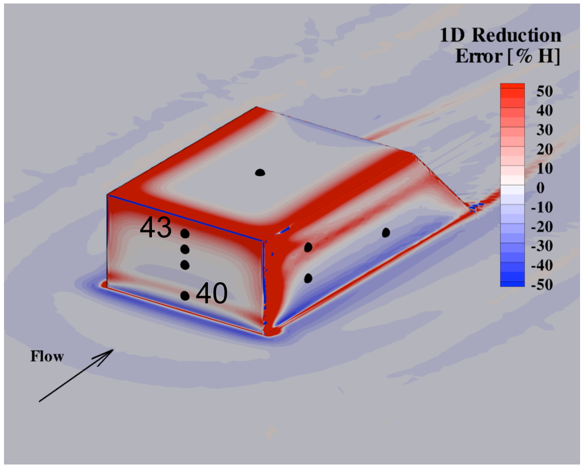

Gage 43: 22%
Gage 40: 10.44%

Without Turntable

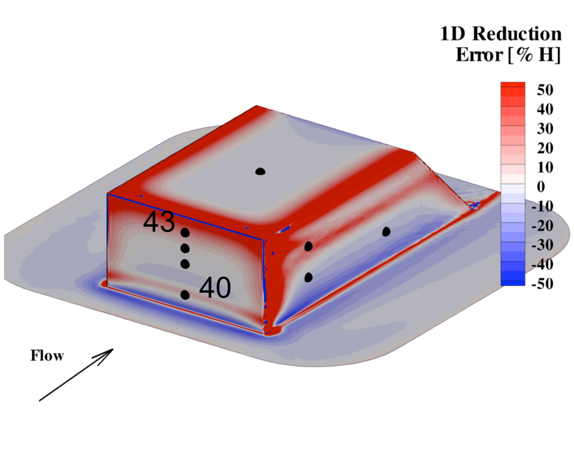

Gage 43: 22%
Gage 40: 10.39%

CFANGLE 0

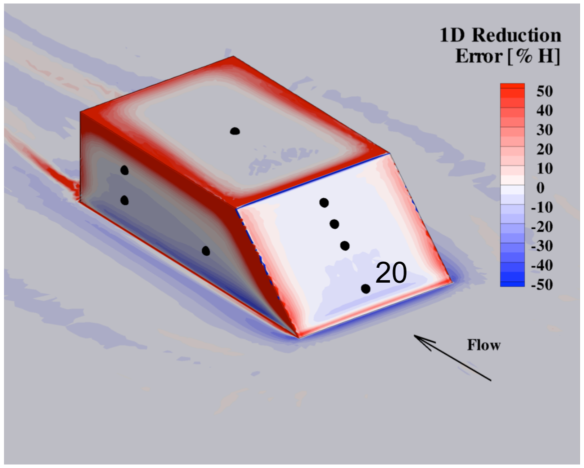

Gage 20: -6.9%

Cylinder vs. Block Protuberances

- **Cylindrical protuberances show slight error due to surface curvature**
  - Could be fixed by computing 1D solution in radial coordinates
- **Similar sensitivity to top surface in the vicinity of the corner**

Model 1

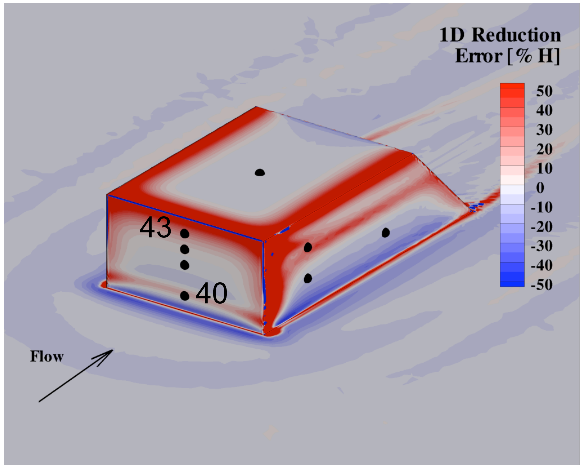

Gage 43: 22%
Gage 40: 10.44%

Model 9

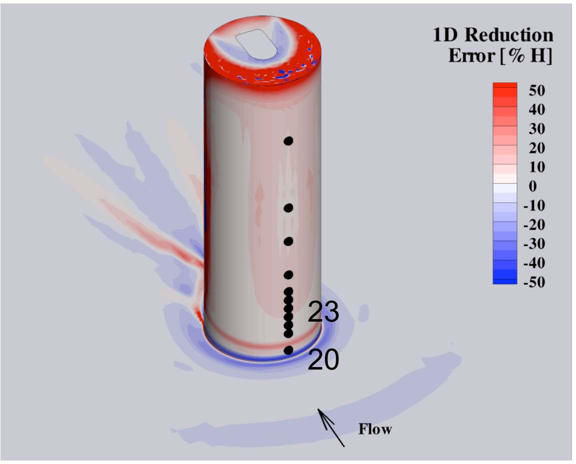

Gage 23: 5.0%
Gage 20: 5.9%

Model 10

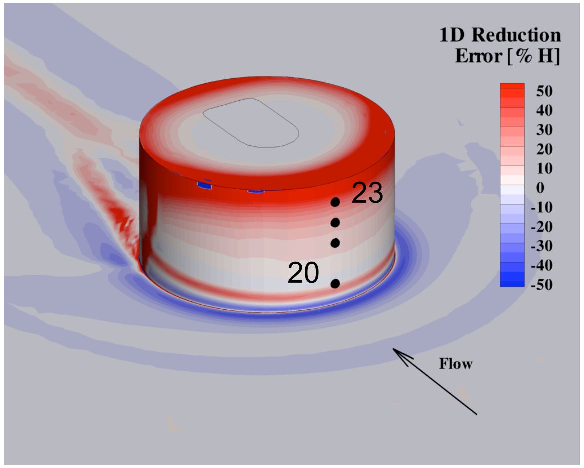

Gage 23: 5.5%
Gage 20: 35%

CFD Conduction Analysis Summary

- **Trends in 1D/3D conduction data reduction error are identified**
  - Errors are typically overprediction errors
  - Errors could be as significant as 40% for some isolated gages
  - Primary conduction mode seems to be influence of ‘sides’ of otherwise 1D surfaces
    - Localized heating features are present, but more difficult to define and are much more dependent on features generated by un-validated CFD turbulence models

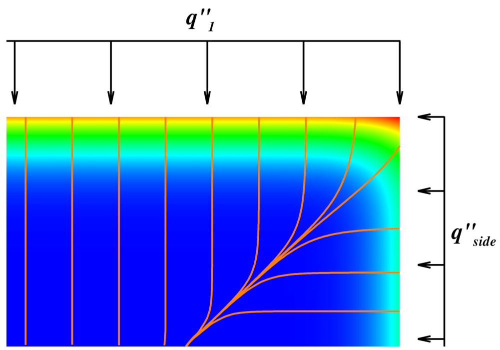

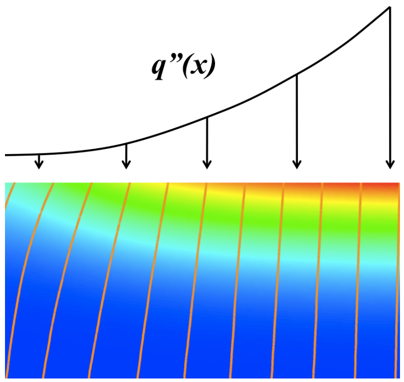

- **Limitations**
  - Since the ‘applied’ heating is based on un-validated CFD, it is possible that turbulence model failings are causing an overstatement of the data reduction error
  - If ‘correction factors’ are computed based on this work, the ‘fixed’ data could not be technically used for CFD validation since CFD defined the corrections

Unit Problems

- **Investigating various conduction loss modes with a 2D flat plate**
- **Thin wall (backface temp rise)**
  - 1D reduction yields accurate answer for short period, then overprediction error rapidly grows
- **Non-uniform (cubic) heating**
  - On higher heating side of profile, 1D reduction yields underprediction that slowly grows in time
- **Side heating**
  - Overprediction error begins very early and grows nearly linearly with time

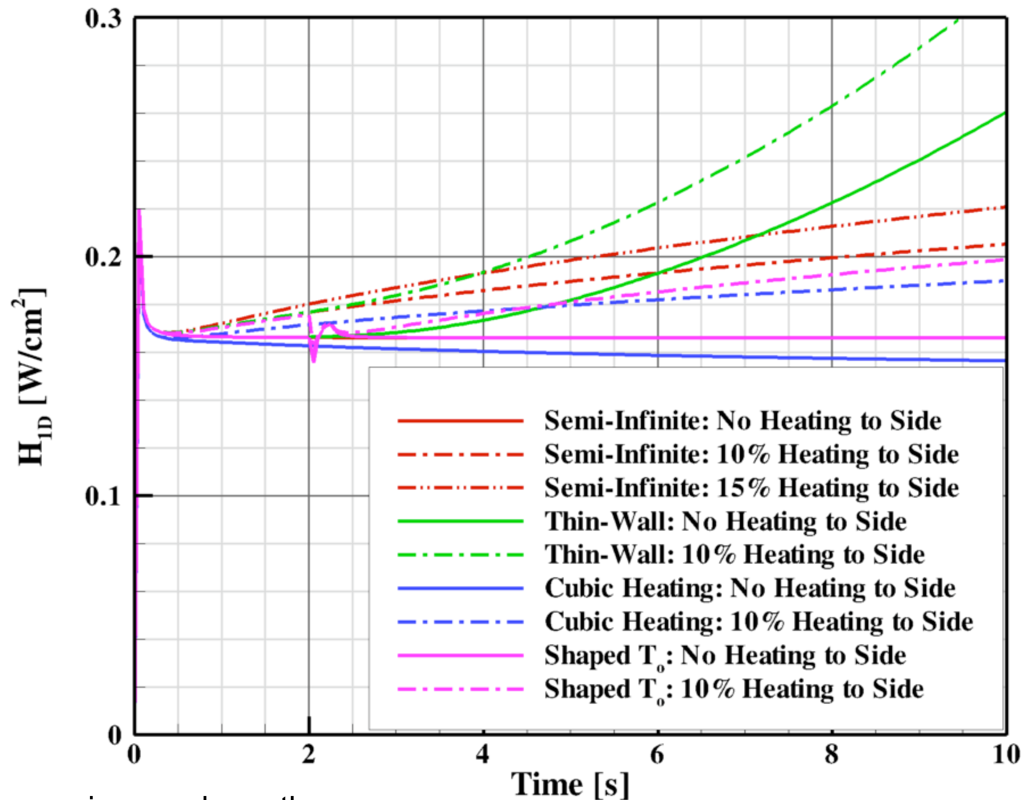

  - When combined with other modes, behaves as if superimposed on other errors
- **Shaped T_o**
  - Small increase in total temperature for first 2 seconds, then up to same level as previous
  - Increase in heat flux at 2 seconds overpowers previous errors for a brief time, but then errors trend to values without slow start

Comparisons to Pretest CFD – Mach 1.5

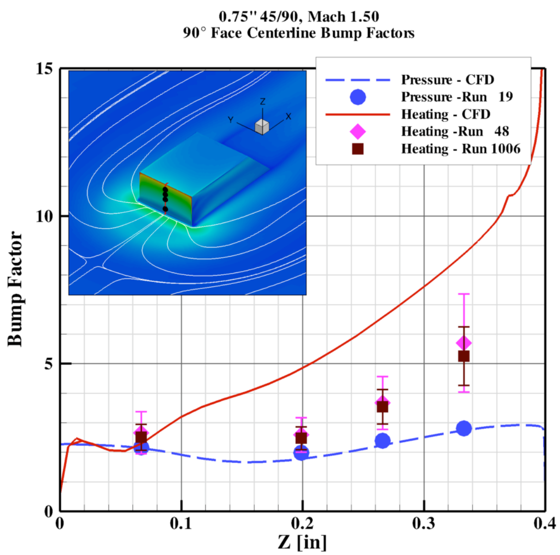

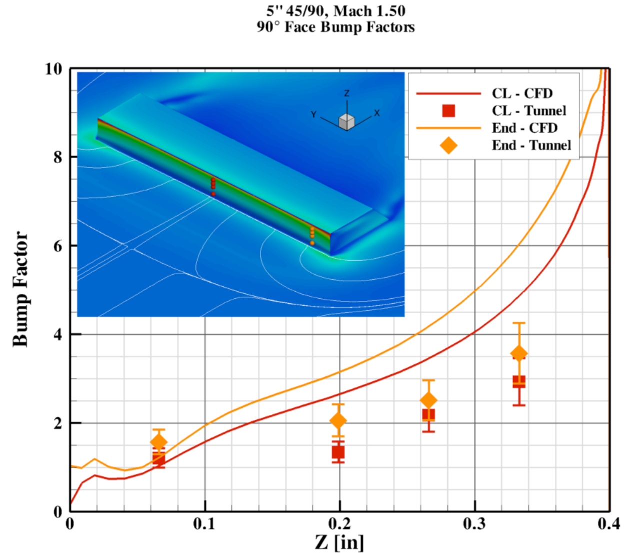

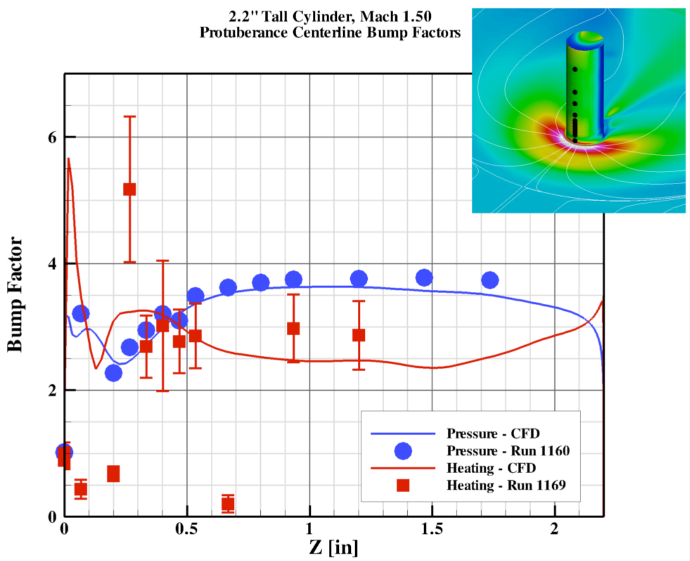

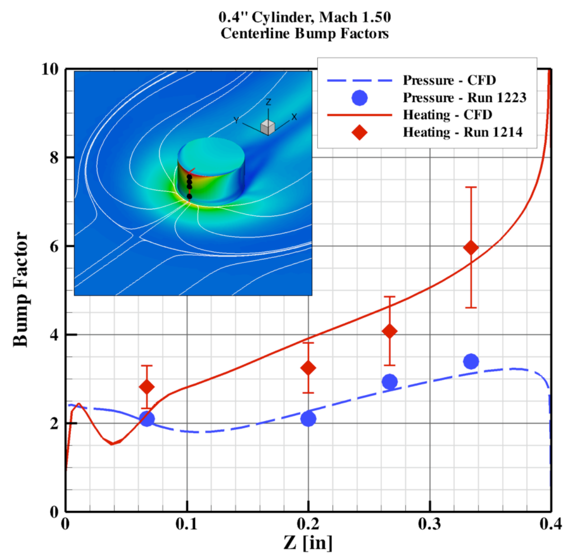

Comparisons to Pretest CFD – Mach 2.16

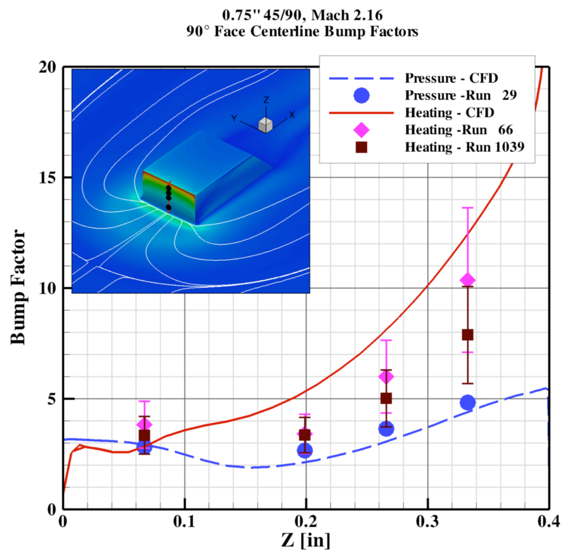

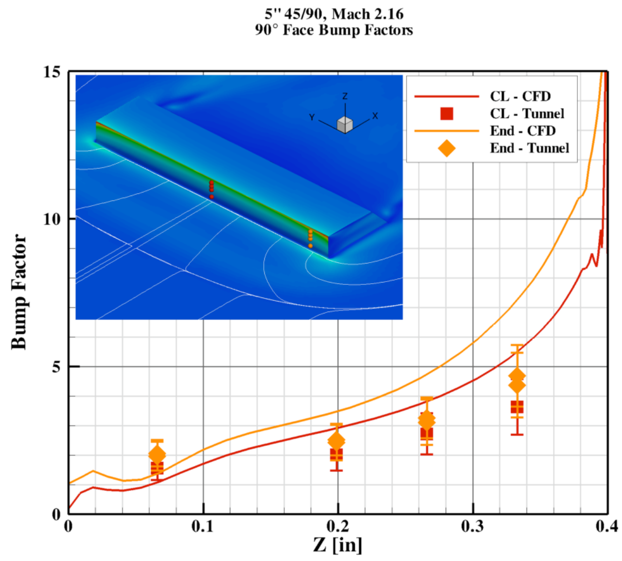

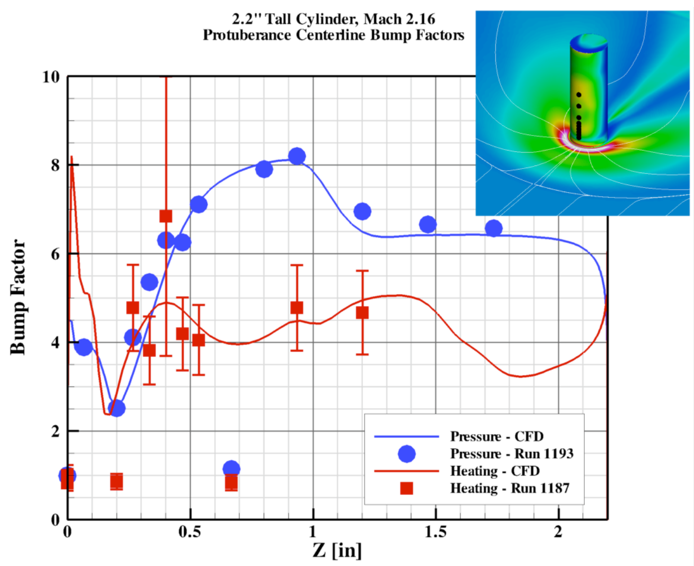

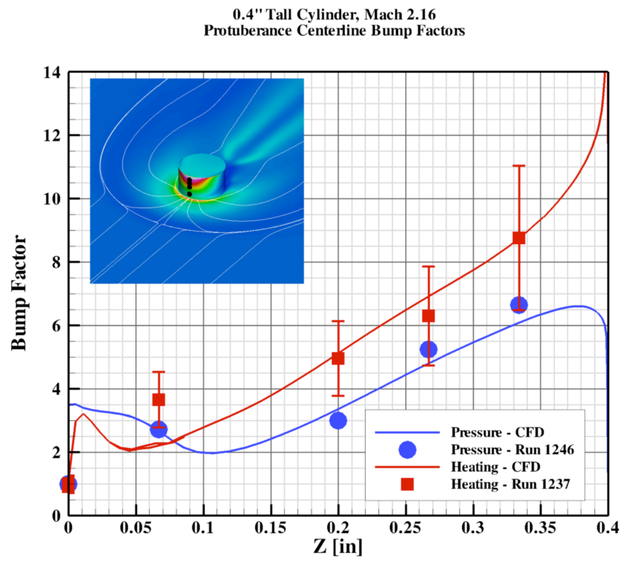

Picking Up the Pieces…

- **The conduction data reduction error is significant, but does not invalidate this dataset**
  - Significant errors are constrained to known gages near sharp changes in geometry
  - Errors tend to be conservative for typical peak-heating gages
  - Correlations which combine the inputs of many gages tends to reduce the influence of errors in a single gages
  - Methods exist and are in development which can provide quantitative estimates of the bias error which can be removed from the data

- **The conduction issue complicates the use of the raw data for model validation**
  - ‘Corrected’ data is only as good as the correction applied
  - Other methods exist for getting the data and model data on similar terms for comparison

Correction Factors

- **Compute a correction factor based on observed reduction error:**

$$\text{Correction Factor} = \frac{\text{Applied Heating}}{\text{Observed 1D Heating}}$$

  - Assumes that error is relatively insensitive to the specific heating levels applied
  - Can check the 'fixed' heating levels by running thermal model and determining if original observation is recovered with the 1D assumption

- **Using tunnel-data as initial 'Applied' heating yielded good results on 90° face, but fell short where less spatial fidelity was built into boundary conditions**

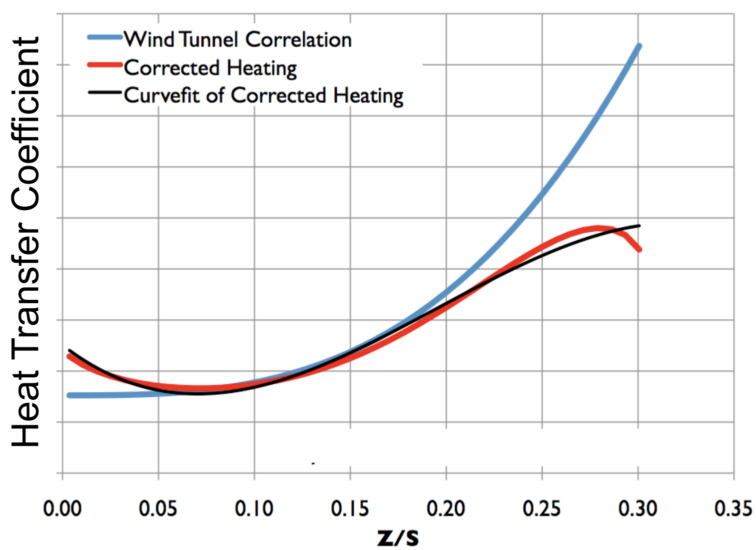

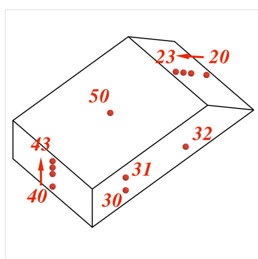

Error in Observed H

Gage	Original BCs	Updated BCs
43	27.7%	0.4%
42	11.5%	3.8%
41	7.3%	7.2%
40	-7.4%	0.8%
31	15.3%	16.9%
50	-7.5%	3.9%
30	0.8%	10.8%
32	-1.3%	7.5%
23	5.5%	23.0%
22	-1.9%	13.1%
21	-3.2%	9.7%
20	-3.7%	5.0%

Thermal analysis based on tunnel data

Correction Factors

- **Using CFD distributions to test the 'Correction Factor' approach yielded better results, but the answer is not perfect**
  - CFD distribution taken as the true applied heating
  - A 3D thermal analysis yielded a set of 'Measured' observations which parallel the thin-film gage measurements
  - Distributions based on the 'Measured' values used to drive a 3D thermal analysis and obtain the '1D Observed' results
  - Comparison between the '1D Observed' and 'Measured' yield a correction factor
  - Correction factor applied to 'Measured' values to yield the corrected estimate of the true heating

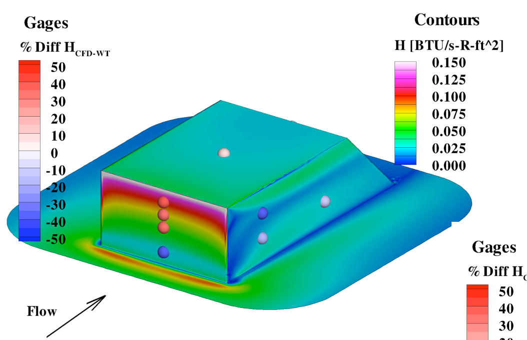

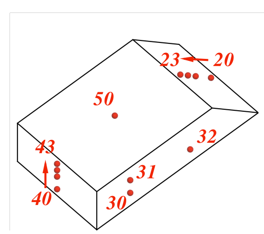

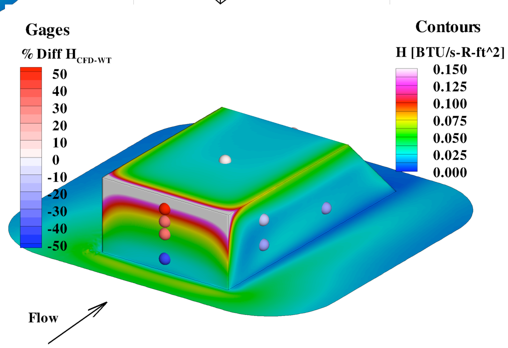

Error in H

Gage	"Measured"	"1D Observed"	Corrected
43	21.9%	27.1%	-4.0%
42	2.5%	4.9%	-2.3%
41	-2.8%	-1.5%	-1.2%
32	-9.6%	-8.3%	-1.4%
50	-3.2%	-2.9%	-0.3%
40	10.3%	-2.2%	12.7%
30	-7.8%	-5.9%	-2.0%
31	25.8%	24.9%	0.8%
20	-7.4%	-11.8%	5.0%
21	-2.6%	-2.7%	0.1%
22	-0.8%	4.7%	-5.3%
23	27.2%	28.7%	-1.1%

Correction Factors

- **A simplified method is being developed which uses analytical solutions of the multi-dimensional heat equation to rapidly generate approximate correction factors without the need for CFD or FE thermal analysis**
  - Based solely on the 'heating to side' mode of 3D conduction
  - Use will be for determining first-order estimate of conduction error
  - Presently includes significant assumptions that eliminate the model for use in correcting data for high-fidelity validation
  - Work is presently directed at adding ability to better represent underprediction estimates due to heat lost to the plate

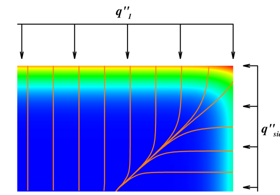

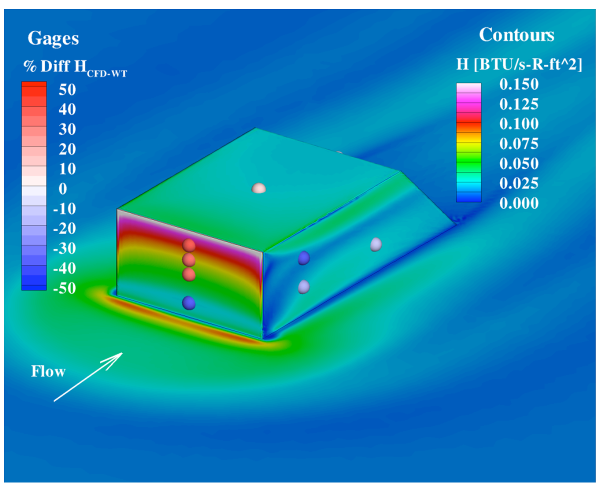

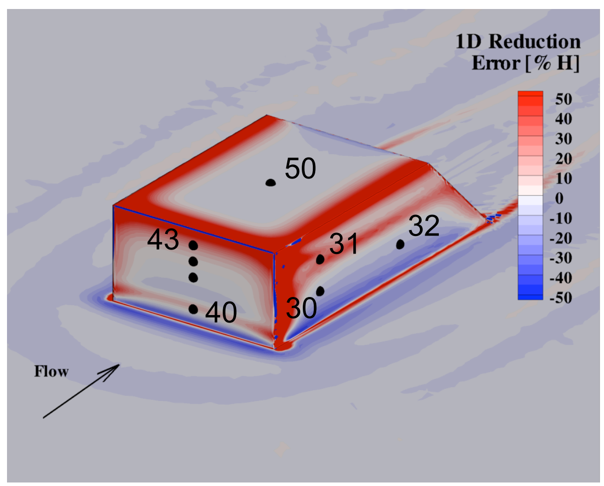

Gage	CFD	Model	Delta
30	1.09	1.05	-0.03
31	0.75	0.91	-0.17
32	1.10	1.05	-0.05
40	0.91	1.19	-0.28
41	1.04	1.00	-0.04
42	0.98	0.95	0.04
43	0.79	0.84	-0.05
50	1.04	1.00	-0.04

Geometries and Grids

Model 1 without turntable: 1.2 million nodes

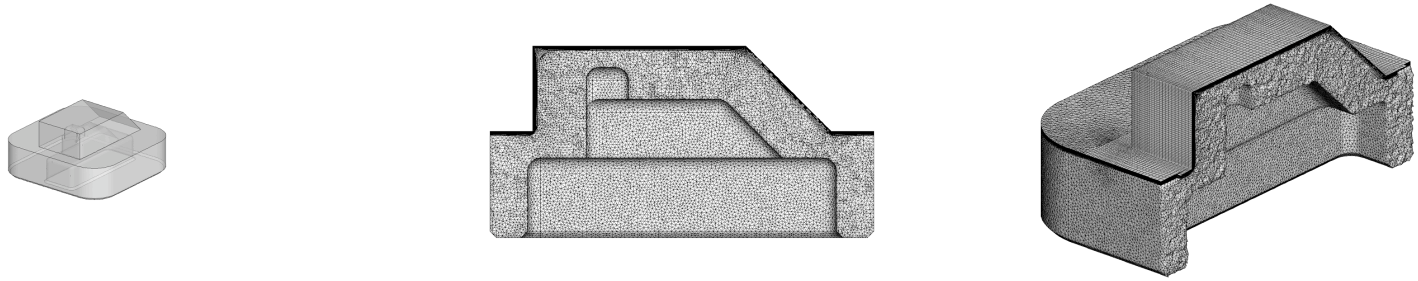

Model 1 with turntable: 1.3 million nodes

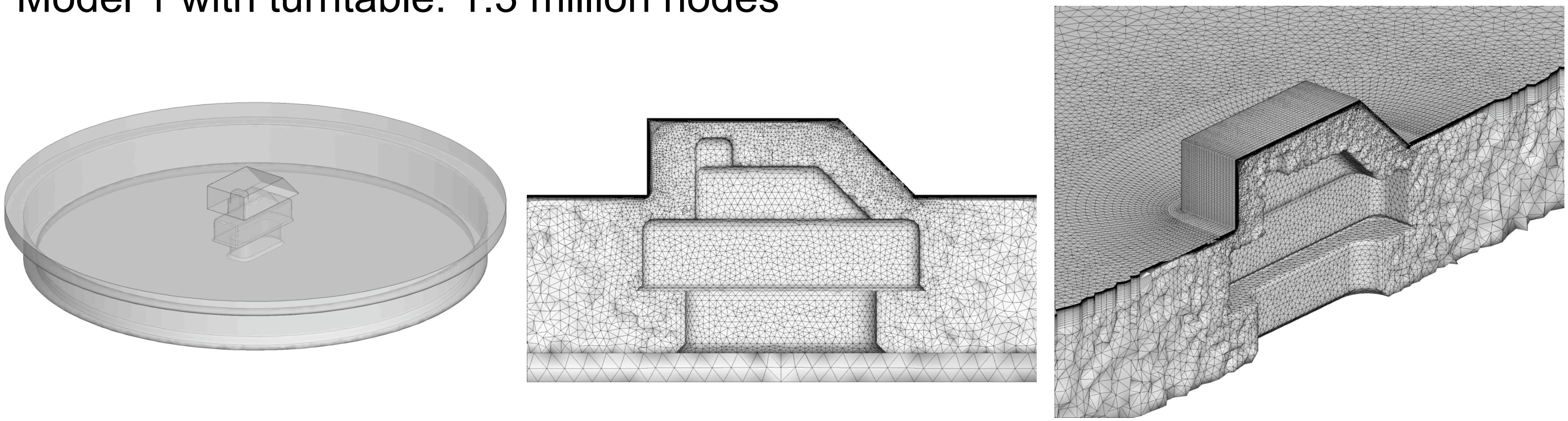

Geometries and Grids

Model 4: 0.95 million nodes

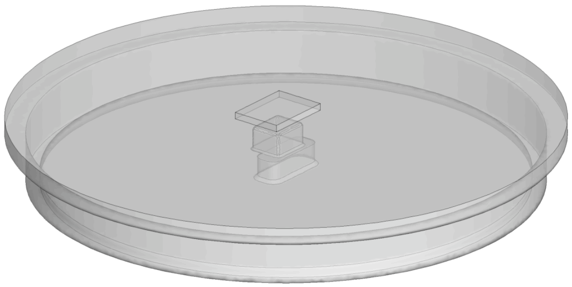

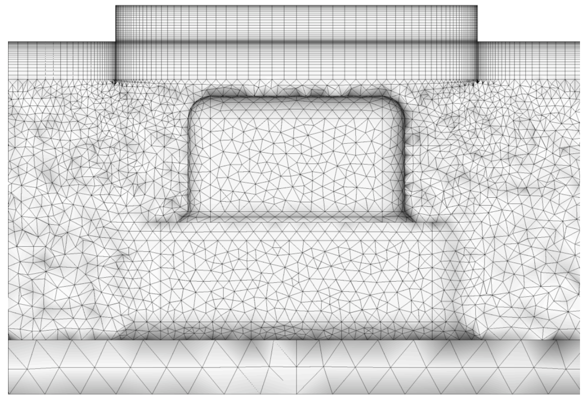

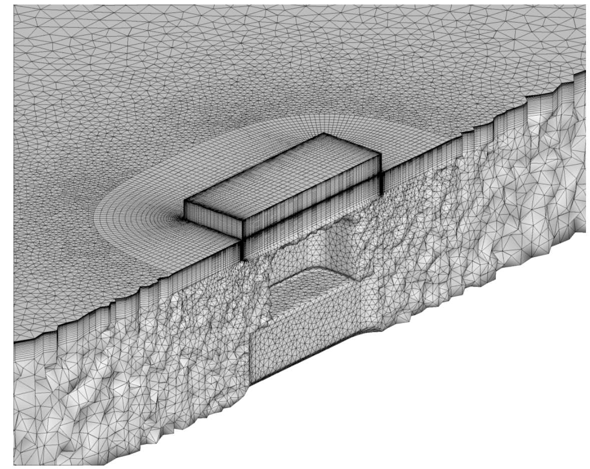

Model 5: 1.2 million nodes

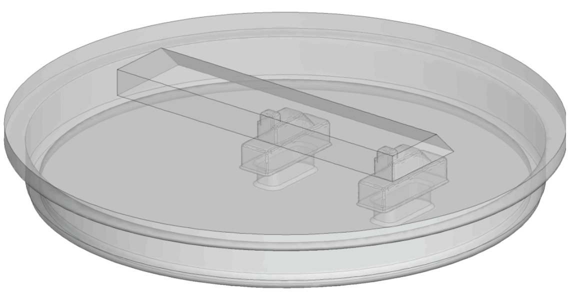

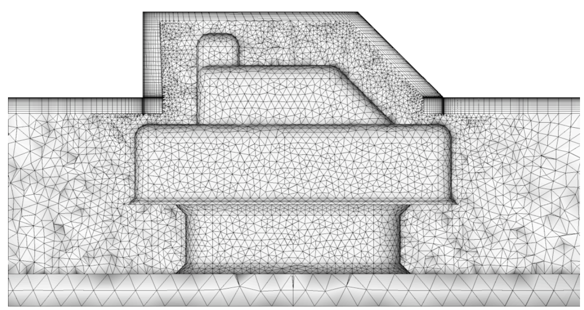

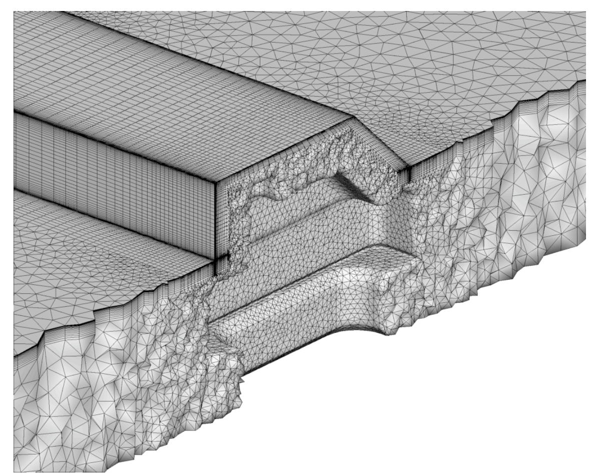

Geometries and Grids

Model 6: 1.4 million nodes

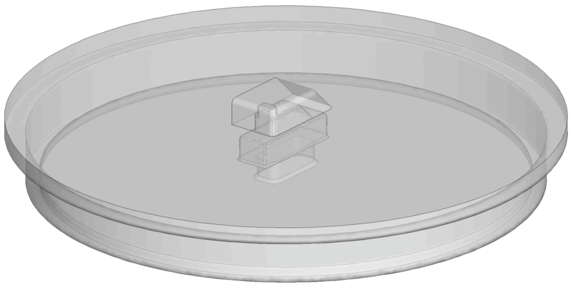
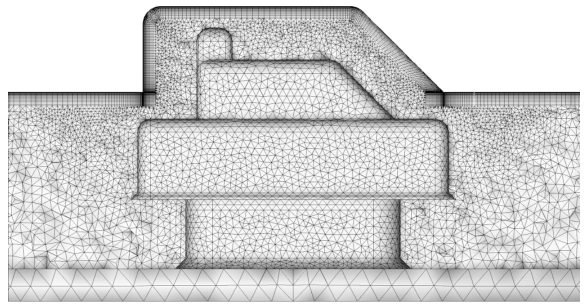
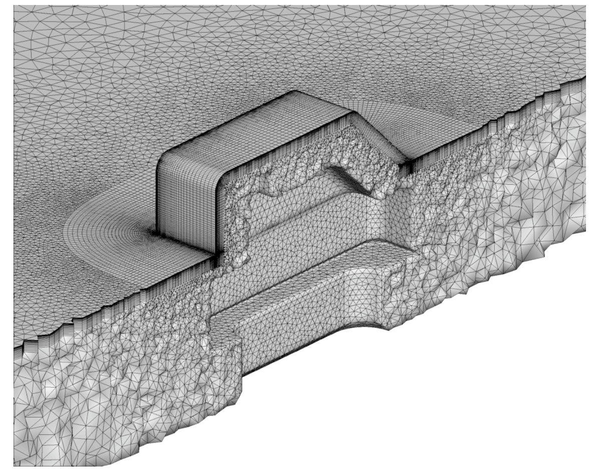

Model 9: 0.67 million nodes

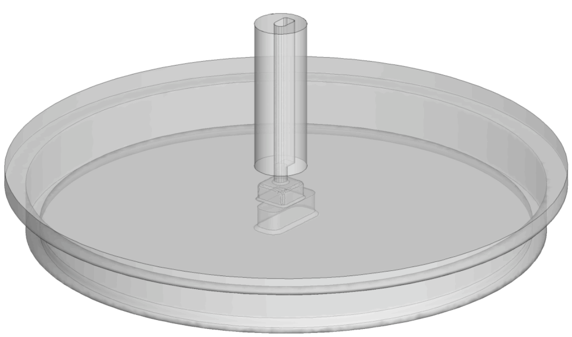
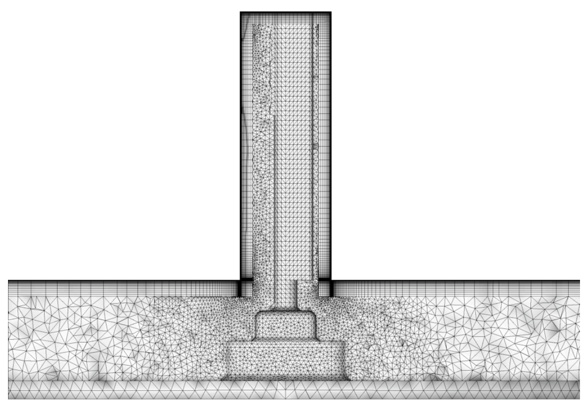
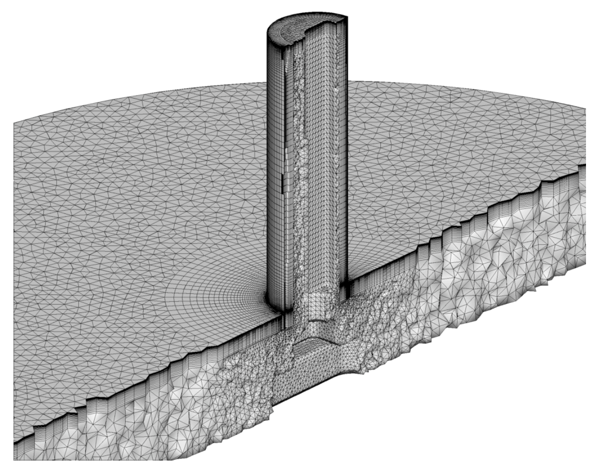

Geometries and Grids

Model 10: 0.52 million nodes

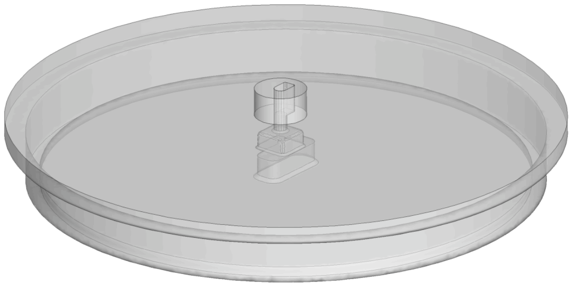
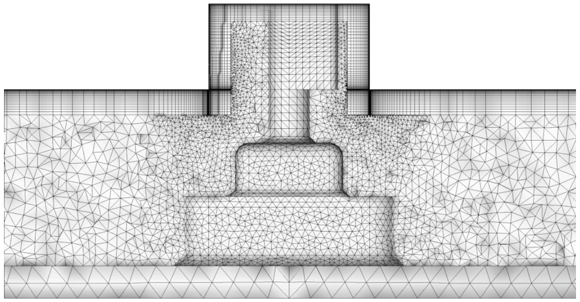
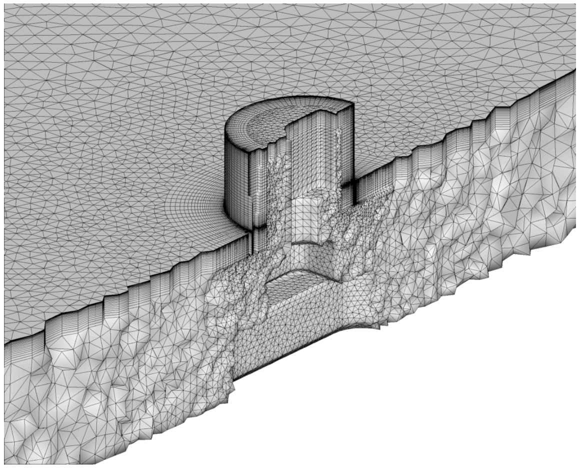

Model 11: 0.89 million nodes